Boundary-layer analysis of a spiral wave core: Spiral core radius and conditions for the tip separation from the core boundary

J. M. Starobin,[1,*] C. F. Starmer,[1,2,3] and A. J. Starobin[1,2,3]

[1]*Department of Physics, University of North Carolina at Greensboro, Greensboro, North Carolina 27412*

[2]*Department of Medicine (Cardiology) and Computer Science, Duke University Medical Center, P.O. Box 3181, Durham,*
North Carolina 27710

[3]*Department of Electrical Engineering, Princeton University, Princeton, New Jersey 08544*

The size of a spiral core is predicted on the basis of a boundary-layer analysis of a spiral tip in the nonkinematic limit. Dependencies of a spiral core radius on medium parameters are found analytically and numerically for two models of excitable media. It is shown that the core radius is determined by the conditions for the tip separation from a core boundary. It is found that a core radius depends on all currents that are active during a wave front formation associated with the diffusion fluxes coupling neighboring elements of excitable media. Varying currents that activated only after wave front formation do not result in a significant altering of a spiral core radius. [S1063-651X(97)51010-5]

PACS number(s): 47.32.Cc, 42.15.Dp, 82.40.−g

For many excitable media, including cardiac tissue, the diffusion fluxes coupling neighboring elements of excitable media reside within the wave front of thickness that is much smaller than the local length of the spiral wave. The dynamics of such waves can be described by the kinematic theory when the wave front radius of curvature is larger than both the wave front thickness and the excitation wavelength [1]. However, this theory is not applicable in some important physiological cases when core radii are smaller than the local wavelength near a spiral wave tip. Such a limit is beyond the assumptions of kinematic theory, since in this case the local radius of curvature is comparable to the wave front thickness and much smaller than the local length of the wave itself [2–4].

Recently we developed a boundary-layer analysis that allowed us to describe an excitation wave tip motion in the limit of large local curvatures. We considered curvatures that were of the order of $1/L_{\text{crit}}$, where L_{crit} was the minimal wave front thickness associated with a nonpropagating plane wave front [2,4]. We found that a spiral wave tip began to meander at the minimal spiral wave core radius which was equal to $L_{\text{crit}}/2$ [4].

In this paper we extend this analysis and introduce the idea that the spiral core size is determined by medium parameters when the tip is not able to maintain its movement along the core boundary.

We focused on modeling with the FitzHugh-Nagumo (FN) class model,

$$\frac{\partial u}{\partial t} = \frac{\partial^2 u}{\partial x^2} + \frac{\partial^2 u}{\partial y^2} + f(u) - V, \qquad (1)$$

$$\frac{\partial V}{\partial t} = \epsilon(\gamma u - V), \qquad (2)$$

where $u(x,y,t)$ is a dimensionless function describing the transmembrane potential in a biological excitable cell and $V(x,y,t)$ is a dimensionless function similar to a slower recovery potassium current. We used a piecewise linear approximation for the current-voltage relationship $f(u) = -\lambda(u - m_1)$ for $u < m_2$ and $f(u) = -\lambda(u - m_3)$ for $u > m_2$. The excitability of tissue was controlled by the slope of $f(u)$, λ, ϵ and by the parameter $\alpha = (m_3 - m_2)/(m_2 - m_1)$ as well. The recovery rate was controlled by the parameter γ. In addition we used the Beeler-Reuter (BR) model [5] to compare our observations with a biologically realistic membrane current kinetics. The BR model consists of a fast sodium current and two potassium currents, the inward rectifier $g\text{K}$, which is always active and the delayed rectifier, $g\text{X}$, which activates only after the action potential is initiated. Thus, we could alter the action potential duration (APD) either independently of wave front formation by varying $g\text{X}$ or simultaneously with wave front formation by varying $g\text{K}$.

Let us consider a spiral core with a circular boundary. Under the assumptions of the conventional kinematic approach [1] one can neglect the wave front thickness and con-
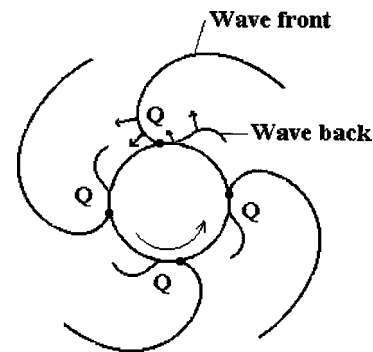

FIG. 1. Rotation of a spiral wave around a circular core boundary in the kinematic limit. The excited region is bounded by an infinitely thin wave front which attaches the infinitely thin wave back at the point Q. This point is an instantaneous center of a spiral tip rotation.

*Author to whom correspondence should be addressed. Electronic address: jmstarob@uncg.edu
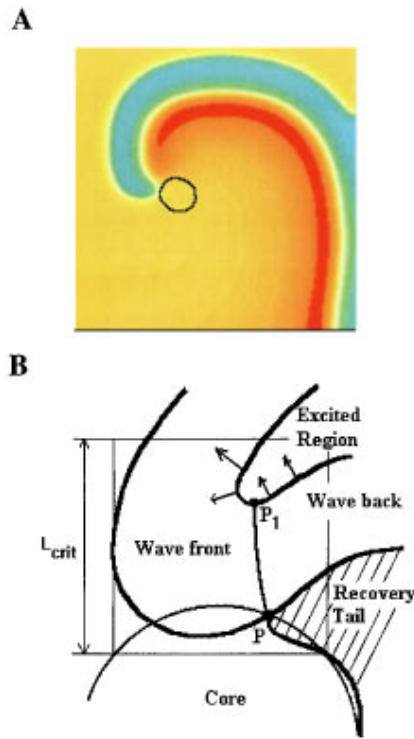
FIG. 2. Spiral wave tip rotation for large tip curvatures which are of the order of L_{crit} (beyond kinematics). (a) (color) demonstrates numerical spiral wave solution of FN model for $\lambda = 0.86$, $\gamma = 7$, $\alpha = 2.76$, and $\varepsilon = 0.018$ (we used a fractional-step implicit method [2,4]). Black circle represents a core boundary. Blue area shows the excited region, thin yellow strip forms the wave front and wave back. Red and reddish areas correspond to a recovery tail. (b) demonstrates tip boundary layer region adjacent to a core boundary. PP_1 is the transition curve where wave front meets wave back and a recovery tail. The segments of wave front and wave back adjacent to PP_1 move in the directions shown by arrows.

sider the excited region of an excitation wave as an area which is bounded by the infinitely thin wave front and wave back. In this case a spiral tip rotates around a circular core and wave front, wave back, and recovery tail meet at point Q as shown in Fig. 1. The rotation of the tip around the point Q is superimposed on the motion along the direction tangential to the core, so at each moment an excitation wave rotates about point Q as about an instantaneous center of rotation. This point has the only velocity component in the direction tangential to the core boundary. The normal component in the direction towards the core center is equal to zero (no-flux core boundary). In this limit, the core radius can go to zero, while the tip curvature goes to infinity [6].

However, for large spiral tip curvatures (core radii which are of the order of L_{crit}) one has to take into account that the wave front and wave back bounding the excited region of an excitation wave have a finite width. Since the tip propagation velocity is very small, one can assume that this width is of the order of L_{crit}, and discretize the tip area by squares with a side which is equal to L_{crit} (Fig. 2) [2,4]. In this limit the excited region attaches to the neighboring wave front and wave back which, unlike a single kinematic point Q, join along the transition curve PP_1. Wave front, wave back, and a recovery tail meet at the point P.

Unlike Q in the kinematic limit, the point P traces a circle
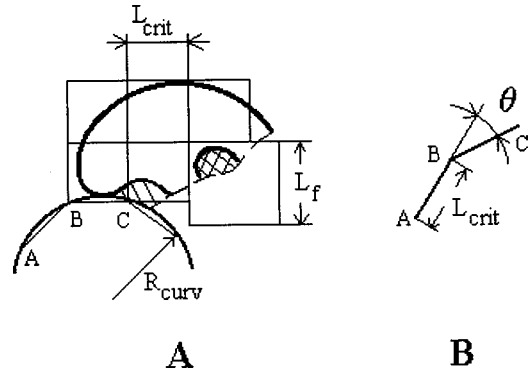

FIG. 3. This demonstrates the rotation of a spiral wave tip around a no-flux circular core boundary. The recovery tail is hatched, an excited region is double hatched. Both the tip and the core boundary are discretized by linear segments L_{crit} (a). The source region of the wave front adjacent to the tip (square with a side of L_f) accumulates charge that flows out into the boundary layer. L_f is the wave front thickness of a straight wave front. (b) shows the angle θ between two adjacent segments of a piecewise linear approximation of the core boundary.

that does not lie entirely in the no-flux region. However, one can complement the tip by a neighboring no-flux core area and shift a tip-core boundary to a chord of the L_{crit} square while providing no additional charge flowing into the tip. The extended tip area includes a core segment located between the line, containing the point P, and a chord of the L_{crit} square (Fig. 2). This method simplifies analytical tip-core no-flux boundary conditions so that no-flux tip-core lines coincide with L_{crit} chords, as shown in Fig. 3(a). These chords form a piecewise linear approximation of the no-flux core boundary. Such an approximation is valid for sufficiently small L_{crit} when $\lambda \sim O(1)$ ($L_{crit} = 2\sigma/(\lambda)^{1/2}$, where $\sigma = 1 + \ln 2$, [2,4]). The angle θ between L_{crit} chords [Fig. 3(b)] determines the conditions for the tip separation from the core boundary. Any given set of medium parameters determines the critical angle θ_{crit} when the tip is not able to maintain its movement along the core boundary with radius R_{core}.

Similar behavior was described in studies of tip separation from a no-flux surface of an unexcitable obstacle that was specified by a no-flux boundary condition along its boundary [2,4]. In these studies we derived an analytical approxima-
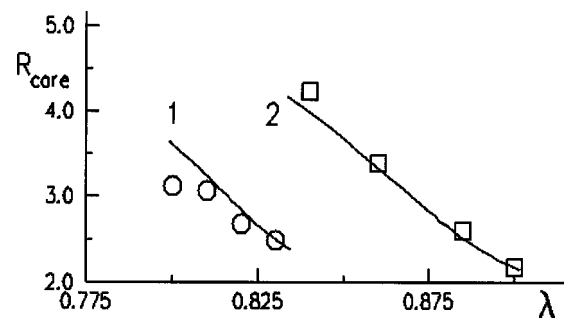

FIG. 4. Dependence of a spiral core radius R_{core} (FN model) on the fast current parameter λ for different γ: $1-\gamma=6$, $2-\gamma=7$ ($\alpha=2.76$, $\varepsilon=0.018$). Circles and squares represent the numerical results. Solid lines represent the analytical analysis [Eqs. (3), (4), and formula (5)].
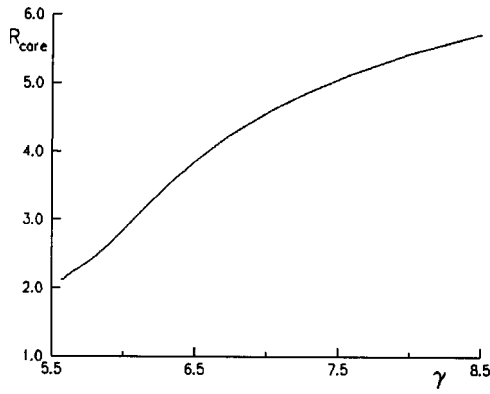
FIG. 5. Dependence of a spiral core radius R_{core} on a slow current parameter γ (analytical predictions, $\lambda = 0.82$, $\alpha = 2.76$, $\varepsilon = 0.018$).

tion describing a tip movement along a piecewise linear unexcitable obstacle and found the conditions associated with the tip separation-no separation transition. Whether the wave tip maintained the attachment or separated from the no-flux boundary depended on the balance of diffusion fluxes obtained by averaging Eqs. (1) and (2).

We averaged the fluxes within a piecewise rectangular approximation of the boundary layer [tip area shown in Fig. 3(a)] over the tip formation time while it extended between the adjacent segments AB and BC [Fig. 3(a)]. From the charge balance and averaging procedures we derived the equation from which one could find the medium parameters associated with the tip separation from the no-flux piecewise linear surface [Eq. (3)],

FIG. 6. Dependence of the APD on the Beeler-Reuter current kinetics. Curves a,b,c,d correspond to $gNa=2.2$ and $gK=0.325$, $gX=4.0$ (meander); $gK=0.35$, $gX=0.8$ (no meander); $gK=0.325$, $gX=0.8$ (meander); $gK=0.35$, $gX=-0.3$ (no meander), respectively. Curve e corresponds to $gNa=3.0$ and $gK=0.35$, $gX=0.8$ (meander).
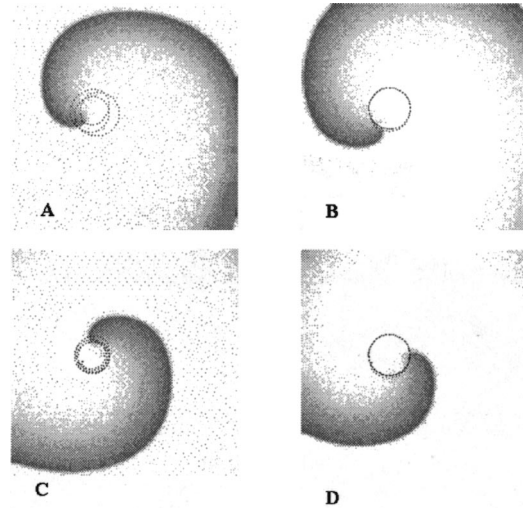

FIG. 7. Behavior of a spiral wave core near meandering transition for the Beeler-Reuter model. (a) $gK=0.325$, $gX=4.0$ (meander); (b) $gK=0.35$, $gX=0.8$ (no meander); (c) $gK=0.325$, $gX=0.8$ (meander); (d) $gK=0.35$, $gX=-0.3$ (no meander). Varying of a delayed rectifier current gX results in significant altering of the APD (Fig. 6). However, a spiral core radius changes insignificantly [(b) and (d)].

$$\left(f_1(\theta) - f_2(\theta) \frac{\alpha+1}{2\sigma^2(\alpha-1)} \right) \lambda^3$$
$$+ f_3(\theta) \left(\frac{(\alpha+1)^3}{4\alpha(\alpha-1)} \lambda^2 - \varepsilon \frac{\gamma(\alpha+1)^5\sigma}{4\alpha^2(\alpha-1)} \right) = 0. \qquad (3)$$

Functions $f_1(\theta)$, $f_2(\theta)$, and $f_3(\theta)$ are determined in [4]. The first and the second functions describe the average angle dependencies of the perimeter and the area of the tip, respectively. The third one describes the area angle dependence of the source wave front region adjacent to the spiral tip [Fig. 3(a)].

The local angle θ between the linear segments of the no-flux boundary can be readily linked to a local curvature radius R_{curv} associated with the local angle apex [Fig. 3(b)]

$$R_{curv} = \frac{L_{crit}}{2\sin(\theta/2)}. \qquad (4)$$

For any given set of medium parameters λ, γ, ε, and α Eqs. (3) and (4) determine the critical angle θ_{crit} and the local radius of curvature $R_{curv}(\theta_{crit})$ associated with the tip separation-no separation transition. The critical angle ranges from π to 0 (Eqs. 3 and 4). The larger θ_{crit} the smaller the radius of curvature associated with separation-no separation transition. When θ_{crit} is equal to π the separation-no separation radius of curvature approaches its minimal value $L_{crit}/2$ [4].

The tip will separate from the no-flux boundary when $R_{curv} < R_{curv}(\theta_{crit})$ and will maintain the attachment to it when $R_{curv} > R_{curv}(\theta_{crit})$. The minimal curvature radius which is associated with the attachment to the no-flux boundary is equal to $R_{curv}(\theta_{crit})$.

Using this analysis for a piecewise linear approximation of a no-flux boundary of a spiral core, one can find the radius of a spiral core, which is given by
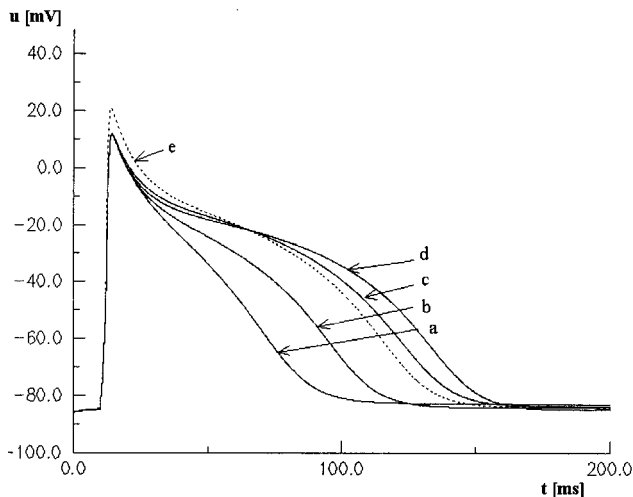
$$R_{\text{core}} \equiv R_{\text{curv}}|_{\theta=\theta_{\text{crit}}}. \tag{5}$$

Formula (5) indicates that a spiral core is bounded by a minimal size circular trajectory when the tip is still able to maintain the attachment to a boundary of a spiral core. Notice that with given medium parameters and $\theta < \theta_{\text{crit}}$ a tip rotation radius is decreasing toward $R_{\text{curv}}|_{\theta=\theta_{\text{crit}}}$ due to the charge imbalance between the boundary layer and adjacent medium. With $R \equiv R_{\text{curv}}|_{\theta=\theta_{\text{crit}}}$ the charge balance is attained. We found that analytical estimation [Eqs. (3), (4), and formula (5)] is in good agreement with numerics (Fig. 4).

Equations (3) and (4) demonstrate that all medium parameters control the boundary layer formation, affecting the area of the tip and the radius of the spiral core [formula (5)]. Dependencies of the core radius on fast and slow current parameters λ and γ are shown in Figs. 4 and 5, respectively. Figure 4 demonstrates the decrease of the core radius when a fast current parameter λ increases. Unlike λ, the increase of the slow current parameter γ results in the increase of the radius of a spiral core (Fig. 5).

The analytical analysis of a spiral wave core developed in the framework of the FN model demonstrates a crucial role of the medium parameters which control a boundary layer formation. However, this two variable model (parameters λ, γ) does not provide information about the relationship between a spiral core and other currents that are not active during wave front formation.

In order to study this relationship we chose the BR model and performed numerical simulations which allowed us to alter the wave front formation independently of the APD. The APD was changed by varying both inward and delayed rectifier currents ($g\text{K}, gX$) (Fig. 6). We focused on the dynamics of a BR spiral core near its meandering transition. Numerical experiments demonstrated that altering the delayed rectifier current gX, which activated after wavefront formation, changed the APD but had minimal influence on a spiral core radius (Figs. 6 and 7).

In summary, we have developed an analytical approach for estimating the size of a small spiral wave core when its radius is of the order of L_{crit}. We have shown that the core radius is determined by the conditions for the tip separation from the core boundary. It is found that the core radius depends on all currents which are active during wave front formation associated with the diffusion fluxes coupling neighboring elements of an excitable medium. Varying currents that activated only after wave front formation do not result in a significant altering of a spiral core radius. This analysis provides new information about reentrant cardiac arrhythmias.

[1] A. S. Mikhailov, *Foundations of Synergetics 1. Distributed Active Systems* (Springer, Berlin, 1990); V. S. Zykov, *Simulation of Wave Processes in Excitable Media* (Manchester University Press, Manchester, 1987).

[2] J. M. Starobin, Y. I. Zilberter, and C. F. Starmer, Physica D **70**, 321 (1994); J. M. Starobin, Y. I. Zilberter, E. M. Rusnak, and C. F. Starmer, Biophys. J. **70**, 581 (1996).

[3] Y. B. Chernyak, A. B. Feldman, and R. J. Cohen, Phys. Rev. E **55**, 3215 (1997).

[4] J. M. Starobin and C. F. Starmer, Phys. Rev. E **54**, 430 (1996); **55**, 1193 (1997).

[5] G. W. Beeler and H. Reuter, J. Physiol. (London) **268**, 177 (1977).

[6] D. A. Kessler and R. Kupferman, Physica D **97**, 509 (1996).